PAPER • OPEN ACCESS

Testing superconducting pairing symmetry in multiterminal junctions

View the article online for updates and enhancements.

Testing superconducting pairing symmetry in multiterminal junctions

T H Kokkeler[1,2,*] ⓘ, A A Golubov[1] and B J Geurts[2,3]

[1] Interfaces and Correlated Electron Systems, Faculty of Science and Technology, University of Twente, PO Box 217, 7500 AE Enschede, The Netherlands
[2] Mathematics of Multiscale Modeling and Simulation, Faculty of Electrical Engineering Mathematics and Computer Science, University of Twente, PO Box 217, 7500 AE Enschede, The Netherlands
[3] Multiscale Energy Physics, Center for Computational Energy Research, Faculty of Applied Physics, PO Box 513, 5600 MB Eindhoven, The Netherlands

E-mail: timkokkeler@gmail.com

CrossMark

Abstract
An approach to distinguish p-wave from s-wave superconducting pairing symmetry and thus to select potential platforms for Majorana fermions is proposed in terms of electronic transport differences in a four terminal junction consisting of superconducting (S) and normal (N) terminals in the diffusive regime. The Keldysh Green's function equations are derived in the θ-parametrisation, incorporating terms previously neglected in the literature. A stable procedure to solve these equations is presented. The supercurrent and differential conductance between two superconducting electrodes were calculated in the Keldysh–Usadel approximation. The N-terminals can be used to manipulate the energy distribution functions of electrons in the junction in order to control the overall charge transport. Our results provide a new experimental test to detect potential p-wave superconductivity. In fact, we show that the differential conductance of junctions containing p-wave superconductors is distinctly different from the differential conductance in junctions with s-wave superconductors, whereas the supercurrent through the junction is qualitatively similar. This is of importance for the search for Majorana fermions since it may help to design experiments to detect signatures of p-wave symmetry, which may lead to potential platforms for Majorana fermions.

Keywords: superconductivity, four-terminal junction, pairing symmetry

(Some figures may appear in colour only in the online journal)

1. Introduction

Ever since the discovery of superconductivity [1], there has been a lot of interest in this phenomenon. Initially, the focus was on the description of bulk superconductors of the so-called conventional or s-wave type [2–4]. Since the prediction [5] and

experimental verification [6] of the Josephson effect, the effect that a DC current can flow through a non-superconducting material sandwiched between superconductors even if no voltage is applied and an AC current flows if a DC voltage is applied, much attention has been paid to the combination of superconductors with other materials, called Josephson junctions. In such junctions the proximity effect plays an important role [7]. Here, proximity refers to the effect that electrons in a normal material close enough to a superconductor become highly correlated in much the same way as inside the superconducting material itself. Research into superconductivity today is not only restricted to conventional superconductors. Since the discovery of anisotropic superconductors [8] and notably

---

* Author to whom any correspondence should be addressed.
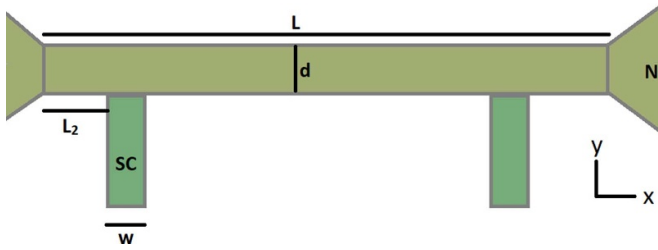
Figure 1. A schematic of the VT junction. Superconducting electrodes (SC) of width w are attached to a bar of length L and width $d << \xi$ between two normal metal (N) reservoirs. The distance between the superconducting electrodes and the normal metal reservoirs is L_2. Free currents can flow between the superconducting electrodes, dissipative currents can flow between either the electrodes or the reservoirs.

the discovery of high temperature superconductors [9], also unconventional superconductors, such as p-wave [10, 11], and d-wave [12] have been investigated. Unconventional superconductors have received even more attention since Kitaev showed that 1D p-wave superconductors may host Majorana particles [13]. In this paper we will concentrate on charge transport in multiterminal junctions composed of normal and superconducting materials in a particular arrangement that promotes the proximity effect. The main finding of this paper is the striking difference in the induced 'differential conductance' between an s-wave and p-wave superconductor. These differences form the basis for possible experimental verification of the type of superconductor one may induce in a particular junction and thus can be used to help identifying materials suitable for possible platforms for Majorana fermions. A typical example of a Josephson junction is the SNS junction, in which a normal metal (N) is sandwiched between two superconductors (S). One way to investigate SNS junctions theoretically is by using Green's functions [14–19]. In equilibrium only the retarded Green's function is studied, for nonequilibrium effects also the Keldysh component is included. Results have been obtained in various approximations, both analytically [20–23] and numerically [24]. In this study, a four terminal variant of the SNS-junction is considered, the VT-junction, first investigated by Volkov and Takayanagi [25–28]. A schematic of the VT-junction is shown in figure 1. Both conventional s-wave and unconventional p-wave superconductors are studied. In s-wave superconductors the so-called superconducting potential, which characterises the strength of the superconducting interactions, is isotropic, in p-wave superconductors the superconducting potential is anistropic. The influence of this anisotropy on physically measurable quantities is theoretically investigated. The diffusive normal metal (N) is considered to be very thin. Therefore, the Green's functions will have only small variation in the lateral directions, so that the problem can be approximated to be one-dimensional following [29]. The interface between the superconductor and the normal metal is modelled using the Tanaka–Nazarov boundary conditions [30–34], which can be used for conventional as well as for unconventional superconductors. The incorporation of these boundary conditions for the VT-junction in equilibrium

was studied in [29, 35]. A new derivation of the equations resulting from these boundary conditions in non-equilibrium VT-junctions is presented for the θ-parametrisation. The VT junction can be used to study the difference between conventional and unconventional superconductors. In [35] the effect on the local density of states was investigated. In [36], a similar approach was used for calculations on the conductance spectroscopy for T-shaped junctions, a three-terminal junction with one superconducting electrode and two normal reservoirs. We develop a self-consistent theory of Cooper pair and quasiparticle transport in the VT structure within the Keldysh–Usadel approach. Our results demonstrate that the differential conductance can be used to distinguish between s-wave and p-wave superconductors. In this, the four terminal characters of the junction will prove to be vital. A voltage will be applied on the normal metal reservoirs, while grounding the superconductors, so that the energy distribution function of electrons in the normal metal can be manipulated, similar to the approach presented in [37]. In this way, the charge transport can be controlled and differences between s-wave and p-wave configurations controlled. In this paper, it is shown that the four-terminal junction can be used to distinguish p-wave superconductors from conventional superconductors, that is, to identify potential hosts for Majorana fermions. The organization of this paper is as follows. In section 2 the Usadel equation is introduced alongside the main approximations made in the theory. In section 3 this theory is used to develop a solution scheme for the problem at hand. In sections 4–7 the results of this scheme are investigated. Finally, concluding remarks are contained in section 8.

2. Usadel equation

The quasiclassical Green's function in a Josephson junction obeys the Eilenberger equation [38, 39]. In the dirty limit, that is, if the coherence length ξ of the Cooper pairs is much larger than the mean-free path l of electron transport, the Eilenberger equation simplifies to the Usadel equation [40]:

$$\mathcal{D}\nabla(G\nabla G) + [-iE\tau_3, G] = 0,$$
$$GG = 1, \tag{1}$$

where 1 is the identity matrix, $\mathcal{D}$ is the diffusion constant, E is the energy of the Cooper pair and $G = \begin{bmatrix} G^R & G^K \\ 0 & G^A \end{bmatrix}$, where $G^R, G^A, G^K \in \mathbb{C}^{2\times2}$ are the retarded, advanced and Keldysh Green's functions respectively. From the Green's functions the density of states ρ, which is the $(1,1)$-element of Re G^R, the spectral supercurrent ImIs $= \frac{1}{2eR_N}\text{Tr}(\tau_3(G^R\nabla G^R - G^A\nabla G^A))$ and the energy distribution functions of the electrons can be calculated. These quantities are at the heart of the investigations into the differences between s-wave and p-wave superconductivity. The superconducting electrodes are incorporated into the model similar to [29]. The two-dimensional Usadel equation is used. Because the normal metal slab is assumed to be very thin, i.e. the distance d in figure 1 is much smaller than the coherence length ξ,

$$\frac{\partial}{\partial y}\left(G\frac{\partial}{\partial y}G\right) \approx \frac{1}{d}\left(\left(G\frac{\partial}{\partial y}G\right)_{y=d} - \left(G\frac{\partial}{\partial y}G\right)_{y=0}\right)$$
$$= -\frac{1}{d}\left(G\frac{\partial}{\partial y}G\right)_{y=0} =: \mathcal{S}(G,x), \qquad (2)$$

where in the second equality it was used that no current flows into the vacuum, that is, $\left(G\frac{\partial}{\partial y}G\right)_{y=d} = 0$, whereas the current from the electrode into the normal metal is $\mathcal{S}(G,x) = S(G)\Theta_S(x)$, where Θ_S is the indicator function of the electrodes. The term S is determined by the Tanaka–Nazarov boundary conditions, which read

$$S = -\frac{1}{d}\left(G\frac{\partial}{\partial y}G\right)_{y=0} = \frac{1}{\gamma_B}[G,B],$$

where γ_B is the ratio of the boundary resistance and the resistivity of N metal multiplied by its coherence length and B is a parameter in the Tanaka–Nazarov conditions discussed in the appendix. The one-dimensional approximation to the Usadel equation reads

$$D\frac{\partial}{\partial x}\left(G\frac{\partial}{\partial x}G\right) + [-iE\tau_3, G] + S\Theta_S(x) = 0,$$
$$GG = 1. \qquad (3)$$

The retarded Green's function can be parametrised using the θ-parametrisation [15],

$$G^R = \begin{bmatrix} \cosh\theta & \sinh\theta e^{i\chi} \\ -\sinh\theta e^{-i\chi} & -\cosh\theta \end{bmatrix}, \qquad (4)$$

where θ,χ are complex functions of the variable x. In the bulk of a superconductor

$$\cosh\theta = \frac{E}{\sqrt{E^2-\Delta^2}}, \qquad (5)$$

$$\sinh\theta = \frac{\Delta}{\sqrt{E^2-\Delta^2}}, \qquad (6)$$

where E is the energy, and Δ is the so-called superconducting pair potential. In s-wave superconductors the pair potential is isotropic, $\Delta = \Delta_0$, in a px-wave superconductor the pair potential has a non-trivial angular dependence, $\Delta = \Delta_0\cos\phi$.

Moreover, it has been shown [39, 41] that the Keldysh Green's function can conveniently and without loss of generality be parametrised as

$$G^K = G^R h - h G^A$$
$$h = \begin{bmatrix} f_L + f_T & 0 \\ 0 & f_L - f_T \end{bmatrix}, \qquad (7)$$

with f_L, f_T real-valued functions of x. The notation f_L, f_T was introduced by [41] to describe what were called longitudinal and transverse modes.

Using the θ-parametrisation and the parametrisation using the distribution functions f_L and f_T, the normalisation condition is automatically satisfied and and only the differential equation remains to be solved.

In this parametrisation, the retarded and Keldysh equations are the solution of

$$\mathcal{D}\frac{\partial\theta}{\partial r^2} = -2iE\sinh\theta + \frac{D}{2}\left(\frac{\partial\chi}{\partial r}\right)^2\sinh\theta + S_\theta\Theta_S(x),$$
$$\frac{\partial}{\partial r}\left(\sinh^2(\theta)\frac{\partial}{\partial r}\chi\right) + S_\chi(\theta) = 0, \qquad (8)$$
$$\nabla(D_L\nabla f_L) + \nabla(C_L\nabla f_T) + \text{Im}s\nabla f_T + \text{Tr}(S^K) = 0,$$
$$\nabla(D_T\nabla f_T) + \nabla(C_T\nabla f_L) + \text{Im}s\nabla f_L + \text{Tr}(\tau_3 S^K) = 0.$$

A derivation of the Keldysh equation in dimensionless form is shown in appendix A, a derivation of the boundary terms in the theta-parametrisation can be found in appendix B. It is shown in the appendix that the terms C_L, C_T are only nonzero if $\text{Im}(\chi) \neq 0$. In the short junction limit, linearisation implies $\text{Im}(\chi) = 0$ throughout the junction. This means that these C-terms can be ignored in the very short junction limit, consistent with [20].

At the reservoirs, boundary conditions are required. In the reservoirs, the Green's function should equal the bulk solution for a normal metal, $G = 1$. For the retarded component this is equivalent to the condition

$$\theta(-L/2) = \theta(L/2) = 0.$$

This requirement does not impose any restriction on χ. A boundary condition for χ can be obtained as follows. Since no supercurrent, that is a current that flows without voltage, should flow into the metal reservoir, there should only be a supercurrent between the electrodes, in the region $-L/2 + L_2 < x < L/2 - L_2$. In the θ-parametrisation, the supercurrent is $\sinh^2\theta\frac{\partial\chi}{\partial x}$. In general, for $-L/2 < x < -L/2 + L_2$ and $L/2 - L_2 < x < L/2$, $\theta \neq 0$. Thus, having no supercurrent means that $\frac{\partial\chi}{\partial x} = 0$ for $x \in (-L/2, -L/2 + L_2)$ and $x \in (L/2 - L_2, L/2)$. This property can be realised by imposing the boundary condition

$$\frac{\partial\chi}{\partial x}(-L/2) = \frac{\partial\chi}{\partial x}(L/2) = 0.$$

For the Keldysh equation, Dirichlet boundary conditions can be used. In the reservoirs, the energy distribution functions f_L, f_T, follow the Fermi–Dirac distribution [42, 43], so [44]

$$f_L(L/2) = f_L(-L/2) = \frac{1}{2}\left(\tanh\frac{E+V}{2T} + \tanh\frac{E-V}{2T}\right)$$

and

$$f_T(L/2) = -f_T(-L/2) = \frac{1}{2}\left(\tanh\frac{E+V}{2T} - \tanh\frac{E-V}{2T}\right),$$

where voltage and temperature are normalised with respect to Δ_0.
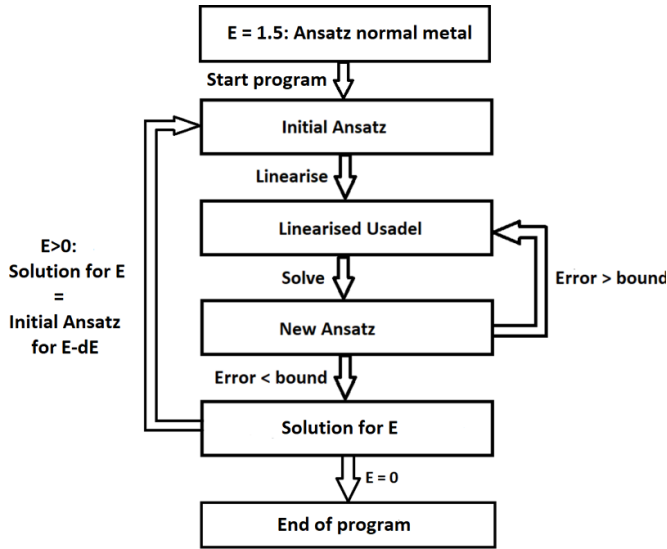
Figure 2. An overview of the computation method used to solve the Usadel equation for a range of energies *E*.

3. Implementation

Following [29], the Usadel equation was recast in dimensionless form using position *x* normalised by ξ and energy normalised by Δ_0 in terms of the coherence length ξ and the superconducting energy gap Δ_0. Here, $\xi = \sqrt{\frac{\mathcal{D}}{2\pi T_c}}$, where $\mathcal{D}$ is the diffusion constant of the normal metal and T_c the critical temperature of the superconducting electrodes. In these units the Usadel equation can be recast as

$$\nabla^2\theta = -2iE\left(\frac{\Delta_0}{2\pi T_c}\right)\sinh\theta + \frac{1}{2}\left(\nabla\chi\right)^2\sinh\theta + S_\theta\Theta_S(x),$$
(9)

$$\nabla\left(\sinh^2(\theta)\nabla\chi\right) + S_\chi(\theta) = 0,$$
(10)

$$\nabla(D_L\nabla f_L) + \nabla(C_L\nabla f_T) + \mathrm{ImIs}\nabla f_T + \mathrm{Tr}(S_K) = 0,$$
(11)

$$\nabla(D_T\nabla f_T) + \nabla(C_T\nabla f_L) + \mathrm{ImIs}\nabla f_L + \mathrm{Tr}(\tau_3 S_K) = 0,$$
(12)

where $\frac{\Delta_0}{2\pi T_c} \approx 0.28$ according to BCS theory [45]. The calculation of the source terms is elaborated on in the appendix. The system of equations (9)–(12) is the system of equations that describes the junction and is to be solved. The retarded equations are nonlinear equations and cannot be solved directly. To solve the retarded equations, an iterative procedure was used. The iterative scheme is shown in figure 2. Equation (10) was linearised around an Ansatz. The resulting equation can be solved using standard discretisation. The solution found to this linearised equation was then used as a new Ansatz until there is convergence. The iteration procedure was started for $\frac{E}{\Delta} = 1.5$. In this energy range, the effect of the superconductors is small compared to the effect for $E < \Delta$, and $\theta = 0$ was used as the first Ansatz. Then, the equation was solved for

Table 1. Parameters of the VT-junction.

Parameter	Value
Nx	101[a]
Ne	221
γ_B	1
z	0.2
$\dfrac{L}{\xi}$	8
$\dfrac{L_2}{\xi}$	1
$\dfrac{w}{\xi}$	0.3
$\dfrac{d}{\xi}$	$\ll 1$
$\dfrac{k_B T}{\Delta}$	0.01[a]

[a] Unless specified otherwise.

successively smaller *E*, using the solution of the equation for energy *E* as the first Ansatz for the equation for energy $E - dE$. It was found that this iterative procedure converged in all cases that were investigated. The Keldysh equations are linear in f_L and f_T, albeit with nonconstant coefficients. A standard discretisation procedure was used here.

4. Differential conductance

Similar to [36], the differential conductance was calculated for the junction. Here all four terminals are to be used, the conductance between the reservoirs depends on the supercurrent between the superconducting electrodes. This experiment can thus not be carried out by a normal SNS junction.

In our setup, a voltage is applied between the two normal electrodes of the VT-junction. The superconducting electrodes are grounded, so that their phase does not depend on time. For the conductance, only dissipative currents are considered, that is, only the contribution of $D_T\nabla f_T$ to the current is taken into account. The differential conductance is given by [46]:

$$R\frac{\partial I}{\partial V} = \int_0^\infty \frac{\partial}{\partial V}f_T(E)D(E)dE$$
(13)

$$D(E) = \left(\frac{1}{L}\int_{-\frac{L}{2}}^{\frac{L}{2}}\frac{dx}{D_T(E,x)}\right)^{-1}.$$
(14)

The expression $D_T = \mathrm{Tr}(1 - \tau_3 G^R \tau_3 G^A)$ was calculated in the θ-parametrisation by direct substitution. The result is

$$D_T(E,x) = \frac{1}{2}|\cosh\theta|^2 + \frac{1}{2}|\sinh\theta|^2\cosh\mathrm{Im}\chi.$$
(15)

In the limit where $\mathrm{Im}\chi = 0$, this reduces to the expression used in [46].

(a) S-wave.

(b) P-wave.

(c) S-wave, selection of results.


(d) P-wave, selection of results.
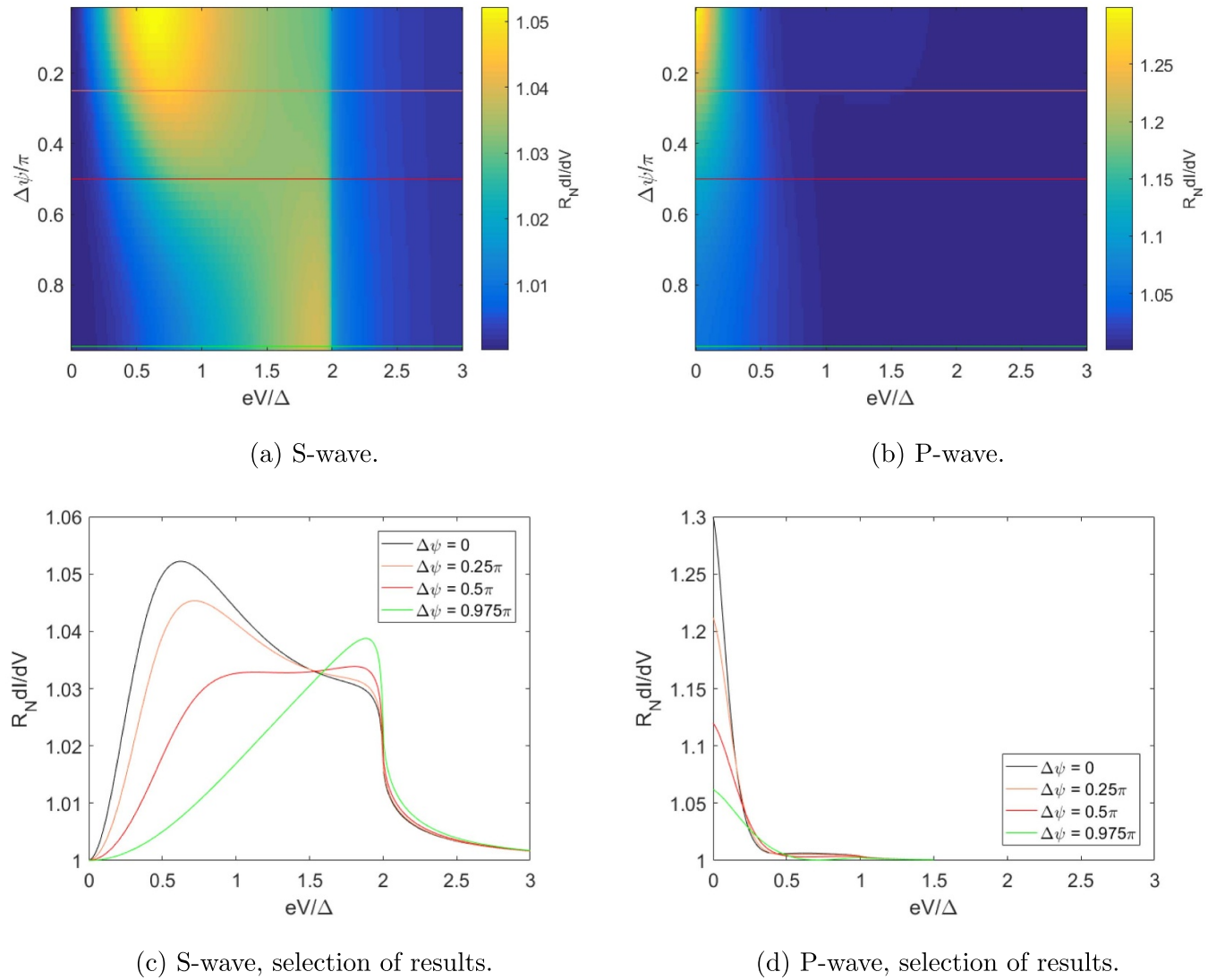
Figure 3. The differential conductance of the VT-junction as a function of the applied voltage between the normal metal electrodes for s-wave (a) and (c) and p-wave (b) and (d) electrodes. For s-wave electrodes, the differential conductance assumes a minimum at $E = 0$, for p-wave electrodes there is a zero bias conductance peak.

In the zero temperature limit, $\frac{\partial}{\partial V} f_T(E) = \delta(E - V)$, and the expression reduces to

$$R_N \frac{dI}{dV} = \left(\frac{1}{L} \int_{-\frac{L}{2}}^{\frac{L}{2}} \frac{1}{\frac{1}{2} |\cosh \theta|^2 + \frac{1}{2} |\sinh \theta|^2 \cosh \operatorname{Im} \chi} dx \right)^{-1} . \tag{16}$$

The phase difference $\Delta \psi$ between the electrodes of the junction was varied. The results for both types of electrodes i.e. s-wave and p-wave are shown in figure 3. The behaviour is qualitatively different for the two types of superconductors. In the case of s-wave electrodes, the differential conductance is lowest at $eV = 0$ and increases with energy to just below $eV = \Delta$. For $\frac{eV}{\Delta} > 1$ the differential conductance approaches the normal state value 1 with increasing energy. With an increase of the phase difference $\Delta \psi$ the dip in the differential conductance becomes broader, the peak appears at increasing $\frac{eV}{\Delta}$, approaching $\frac{eV}{\Delta} = 1$ as the phase difference between electrodes

approaches π. For p-wave electrodes the differential conductance is quite different, as it is lowest at a value $0 < \frac{eV}{\Delta} < 1$ that increases with $\Delta \psi$. As $\Delta \psi$ increases the peak in the differential conductance near $\frac{eV}{\Delta} = 0$ becomes smaller, but broader, so that results for $\frac{eV}{\Delta} > \frac{1}{2}$ only have a very slight dependence on phase. The dependence of the conductance on the phase difference can be understood best from the cases $\Delta \psi = 0$ and $\Delta \psi = \pi$. If $\Delta \psi = 0$ the electrodes are the same and the parameter θ is an even function of position. If however, the phase difference is π, the parameter θ is odd and at the middle of the junction the normal state is attained. Thus, if the phase difference is close to π the proximity effect is suppressed more compared to the case in which the phase difference is close to 0. Since for large E the θ-parameter at the center of the junction is small in any case, this effect is most apparent in the Usadel equation at low energies. Therefore, the deviation of the conductance at low voltages will be smaller if the phase is closer to π, implying a decrease of the zero bias conductance peak
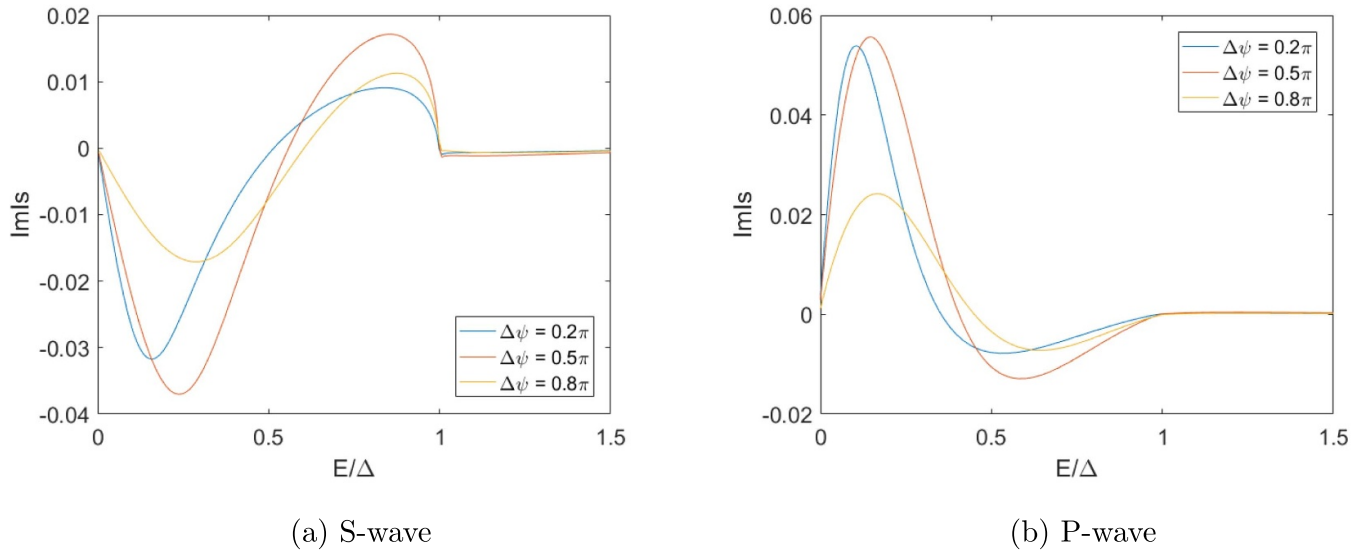
(a) S-wave

(b) P-wave

Figure 4. The spectral supercurrent through the VT-junction as a function of energy for s-wave (a) and p-wave (b) electrodes. The spectral supercurrent changes sign as energy is increased for both s-wave and p-wave electrodes. For clarity of presentation, a selection of the results is shown. An overview of all results is shown in the appendix.

for the p-wave case and a broadening of the dip for the s-wave case. If the phase difference between the electrodes vanishes, the differential conductance is similar to the differential conductance as found in [36], as expected.

5. Spectral supercurrent

The spectral supercurrent ImIs (E,x), [20], is the energy dependent quantity that indicates the current carried by the levels at a given energy if these levels are occupied. The spectral supercurrent is defined as

$$\text{ImIs} = \text{Tr}\left(\tau_3(G^R \nabla G^R - G^A \nabla G^A)\right) \tag{17}$$

$$= \text{Tr}\left(\tau_3 G^R \nabla G^R - (\tau_3 G^R \nabla G^R)^\dagger\right). \tag{18}$$

In the θ-parametrisation this becomes $\text{ImIs} = -4$ Im $\left(\sinh^2\theta \frac{\partial \chi}{\partial x}\right)$. This quantity can be calculated using only the retarded equation. The spectral supercurrent has been calculated for both s-wave and p-wave superconductors as a function of energy and phase. The results are shown in figure 4. Note that the sign of spectral supercurrent for p-wave electrodes is arbitrary, a rotation of π of the electrodes will introduce an extra minus sign in the spectral supercurrent. This can thus not be used to distinguish s-wave and p-wave superconductors.

For both s-wave and p-wave superconductors, there are two extrema in the spectral supercurrent, the maximum spectral supercurrent in the low energy peak being clearly larger than the maximum spectral supercurrent in the higher energy extremum. The low energy extremum occurs at $\frac{E}{\Delta} < \frac{1}{2}$, the high energy extremum at $\frac{E}{\Delta} > \frac{1}{2}$, the exact location of the extremum depends on the phase difference between the electrodes. The appearance of two extrema is a length dependent phenomenon, and will be discussed in more detail in section 7.

The energy of both extrema was investigated for s-wave and p-wave. The results are shown in figure 5. For the low energy extremum, the energy dependence of the extremum on $\Delta\psi$ is smaller for p-wave case electrodes than for s-wave electrodes. For both types of electrodes the extremum energy is non-decreasing as a function of $\Delta\psi$, with the increase slowing down as $\Delta\psi$ increases. However, this process is qualitatively different between s-wave and p-wave electrodes. For s-wave electrodes the increase gradually slows down, for p-wave electrodes the extremum energy becomes approximately constant for $\frac{\Delta\psi}{\pi} > \frac{1}{2}$. For the second extremum the variation is much larger in the p-wave case. As for the first extremum the behaviour between s-wave and p-wave superconductors is different. For s-wave superconductors there is a monotonic increase of extremum energy with $\Delta\psi$. For p-wave electrodes, there is a minimum at around $\frac{\Delta\psi}{\pi} \approx 0.3 - 0.4$. From this we can conclude that the behaviour of the extrema can be used to detect p-wave superconductivity.
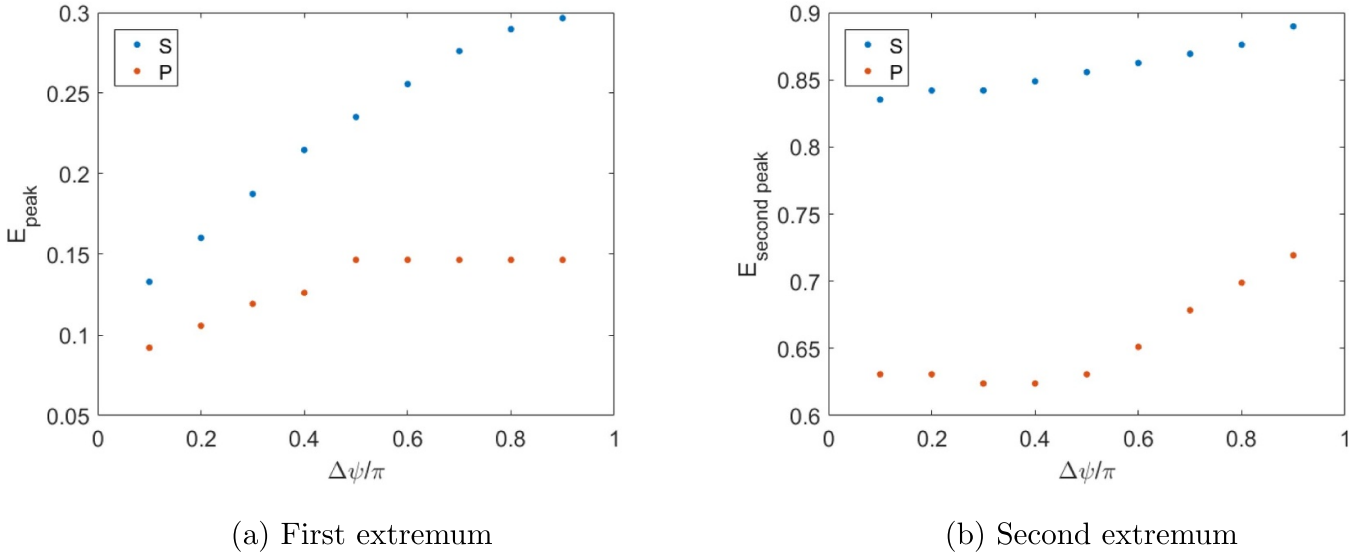
6. Supercurrent

The spectral supercurrent has the disadvantage that it is not directly measurable. A quantity that can be measured in experiment is the total supercurrent. The total supercurrent can be expressed as

$$I_s = \frac{1}{eR_N}\int_0^\infty f_L(E)\text{ImIs}(E)dE, \tag{19}$$

where f_L is the parameter used in the parametrisation of the Keldysh equation, e is the charge of the electron, and R_N is the normal state resistance of the junction [20]. Also the supercurrent will be used in dimensionless form,

$$I_s = \int_0^\infty f_L\left(\frac{E}{\Delta}\right)\text{ImIs}\left(\frac{E}{\Delta}\right)d\frac{E}{\Delta}. \tag{20}$$

(a) First extremum

(b) Second extremum

Figure 5. The energy of the first (a) and second (b) extremum in the spectral supercurrent as a function of phase for the VT-junction using s-wave and p-wave electrodes. There is a qualitative difference between the results. Calculations for $\Delta\psi > \frac{\pi}{2}$ were also calculated using a grid with 401 grid points instead of 101 grid points. This gives the same extremum locations.
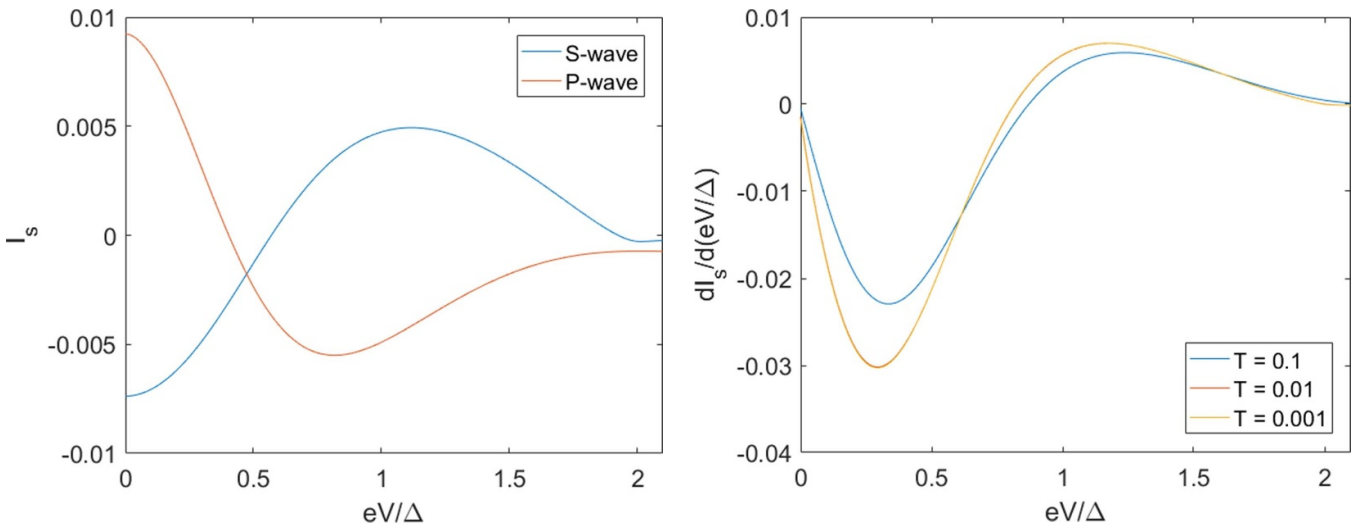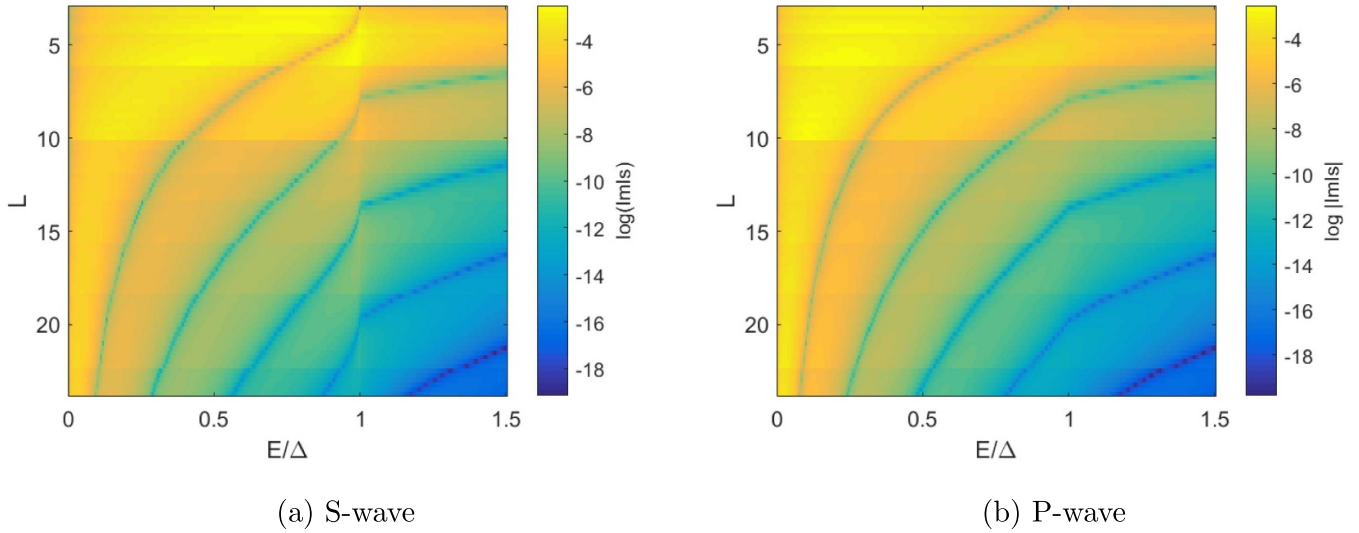

Figure 6. The supercurrent as a function of voltage for the VT-junction in case of s-wave and p-wave electrodes. As for the spectral supercurrent there is a sign difference in the supercurrent between the case of s-wave and p-wave electrodes.

Figure 7. The derivative of the supercurrent with respect to the voltage for the VT-junction for different temperatures. Temperatures have been normalised to $\frac{\Delta}{k_B}$. The results for $T = 0.01$ and $T = 0.001$ are almost equal, and correspond well with the spectral supercurrent for $T = 0.1$ the results are clearly different.

The boundary conditions for the Keldysh equation are determined by the voltage applied between the normal metal reservoirs, as discussed in section 2. These boundary conditions are temperature dependent. In the following calculations, the low temperature regime was investigated, using $\frac{k_B T}{\Delta} = 0.01$. As for the differential conductance, a voltage is applied between the normal metal electrodes, whereas the superconducting electrodes are grounded. The Keldysh equation has been solved for both s-wave and p-wave superconductors. The supercurrent calculated from the results is shown in figure 6. The supercurrent shows a peak at zero voltage level, and decreases and changes sign as the voltage between the reservoirs is increased.

There is a second, lower, peak at larger voltages. This is in good correspondence with the results found in [37]. As expected from the results for the spectral supercurrent, the results of the s-wave and p-wave superconductors differ in sign. A derivative of the supercurrent can be taken with respect to the voltage applied between the reservoirs. The so-obtained quantity $\sigma = \frac{\partial I_s}{\partial \frac{eV}{\Delta}}$ is shown in figure 7. In the low temperature regime, σ is very similar to the spectral supercurrent. This can be explained from the energy distribution functions of electrons for the normal reservoirs. At temperatures $T << \Delta$, the hyperbolic tangent is very similar to the sign function,

(a) S-wave

(b) P-wave

Figure 8. The spectral supercurrent as a function of energy and length of the junction. For clarity of presentation, it was chosen to use $\log \mathrm{ImIs}$. For both s-wave and p-wave electrodes, the number of zeros in ImIs increases as the length of the junction is increased.
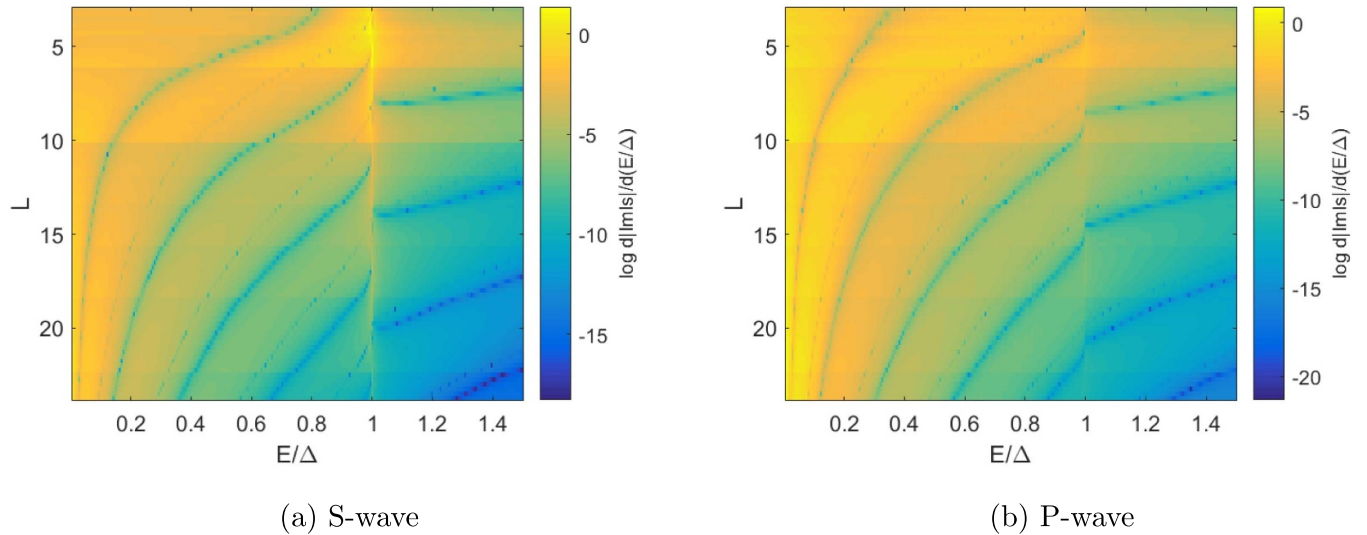
(a) S-wave

(b) P-wave

Figure 9. Derivative of spectral supercurrent with respect to energy as a function of energy and length of the junction. Again, a logarithmic plot was chosen. In the case of s-wave electrodes there is only a discontinuity at $E = \Delta$. For p-wave electrodes, the discontinuity at $E = \Delta$ is less apparent then for s-wave electrodes, and a discontinuity at $E \approx \frac{\Delta}{4}$ is visible for all lengths. This corresponds to the kink observed in previous sections.

being -1 for negative arguments and 1 for positive arguments. This means that f_L is zero in the range $|E| < eV$, and nonzero outside this range. In the region between the superconductors the exact form of f_L will be different, but if the effect of the superconductors on f_L is not too large, the supercurrent can be approximated by

$$I_\mathrm{s} \approx \int_{\frac{eV}{\Delta}}^{\infty} \mathrm{ImIs}\left(\frac{E}{\Delta}\right) d\frac{E}{\Delta}, \qquad (21)$$

$$\sigma \approx -\mathrm{ImIs}. \qquad (22)$$

7. Length dependence of spectral supercurrent

The calculations for $\Delta\psi = \frac{\pi}{2}$, were repeated for other junction lengths to investigate the length dependence of the spectral supercurrent. The results are shown in figure 8. For both s-wave and p-wave electrodes, the number of zeros of the spectral supercurrent increases as the length of the junction is increased. This is due to the larger variation of the complex argument of θ if the length of the junction is varied, as illustrated in appendix C. This is analogous to the ballistic junction, where multiple Andreev bound states are observed for long junctions [19, 47, 48]. A small difference difference between s-wave and p-wave superconductors becomes more apparent if the energy derivative of ImIs is investigated, as in figure 9.

For both types of superconductors there is a discontinuity at $E = \Delta$, but this discontinuity is much more apparent in the s-wave case than in the p-wave case. The results away from $E = \Delta$ are qualitatively similar, although from figure 9 it is clear that peaks in the spectral supercurrent occur at lower voltages if p-wave superconducting electrodes are used compared to if s-wave superconducting electrodes are used. This is in good correspondence with figure 5.

8. Conclusion

In this paper a method has been developed that extends the solution method for the Usadel equations in the VT junction, using Tanaka–Nazarov boundary conditions, to non-equilibrium systems. The Usadel equation was derived in most general form for non-equilibrium superconductivity, allowing for a complex parameter χ. New terms were identified in the equations for the Keldysh components. It was shown that the equations reduce to the known equations if the parameter χ can be assumed real. It was shown numerically that in the VT junction the imaginary part of χ does not vanish in general, showing the necessity of these terms. The Usadel equation was supplemented by the Tanaka Nazarov boundary conditions, which can be used for both conventional (s-wave) and unconventional (p-wave) superconductors. The equations resulting from these boundary conditions were derived in the θ-parametrisation. Also the boundary conditions were derived in general form, allowing for a complex parameter χ, and a discontinuity of both parameters along the interface. The expressions found were cast in such a form that the computation is stable. The implementation boundary conditions were tested on a few problems for which analytical approximations are known. The results compared favourably to known theories. Differential conductance and supercurrent were investigated as a function of the imposed phase difference between the electrodes. For the supercurrent, also a length analysis was performed. In this paper, a method has been proposed to distinguish between s-wave and p-wave superconductors. Since the latter are potential hosts for Majorana fermions, the results presented in this article contribute to the search for Majorana fermions. The four terminal characters of the VT junction was exploited to study the effect of applying a voltage to the normal reservoirs. It was shown numerically that the derivative of the total supercurrent with respect to this voltage is approximately equal to the spectral supercurrent at low temperatures. The code developed allows for several extensions. Apart from s-wave and p-wave superconductors, also d-wave and f-wave superconductors can be investigated. Moreover, the normal metal in the can be replaced by a ferromagnetic material or a topological insulator. For this latter I'm adjustment, the Tanaka Nazarov boundary conditions need to be adjusted to give a good description of the spin–orbit coupling. This is an interesting direction for future research. If the normal metal is replaced by a ferromagnetic material adjustment of the Tanaka Nazarov boundary conditions is not needed. The code allows as well for an adjustment of the geometry to multiterminal junctions with more than four terminals. This would allow for a more elaborated investigation of the influence of the geometry on the local density of states and the supercurrent. An extension of the code to solve the two-dimensional Usadel equation would provide an even larger flexibility in the geometry. Another interesting research direction is to drop the dirty limit assumption and use the Eilenberger equation, the quasiclassical equation that is valid also beyond the dirty limit approximation. In this way a greater variety of junctions can be considered. It would be interesting to show that the results of the Eilenberger do coincide with the results of the Usadel equation in the dirty limit for the VT-junction. Next to this, one might consider to solve the full Gorkov equation and investigate in detail the error of the quasiclassical approximation.

Data availability statement

The data that support the findings of this study are available upon reasonable request from the authors.

Acknowledgments

Appendix A. Keldysh equation

In this section the equations for the Keldysh equations will be calculated. It will be shown that in case a complex superconducting phase χ in the normal layer is allowed, additional terms occur compared to expressions previously noted in literature [15, 20]. Recall that the Usadel equation reads

$$\frac{\partial}{\partial x}\left(G\frac{\partial G}{\partial x}\right) + i\epsilon[G, \tau_3] + 2\Theta_S[G, B] = 0. \tag{A1}$$

Moreover, for any matrix Z consisting of a retarded, advanced and Keldysh components we can write $Z_K = Z_R h - h Z_A$ where h is a diagonal matrix. In the following chapters, h will be used in the normal metal, whereas h_s will be used in the superconducting electrodes. First the Keldysh component of the first term will be calculated.

$$
\begin{aligned}
(G\nabla G)_K &= G_R \nabla G_K + G_K \nabla G_A \\
&= G_R \nabla (G_R h - h G_A) + (G_R h - h G_A)\nabla G_A \\
&= G_R \nabla G_R h + G_R^2 \nabla h - G_R \nabla h G_A - G_R h \nabla G_A \\
&\quad + G_R h \nabla G_A - h G_A \nabla G_A \\
&= \nabla h - G_R \nabla h G_A + G_R \nabla G_R h - h G_A \nabla G_A.
\end{aligned}
\tag{A2}
$$

Thus, the Keldysh equation reads

$$
\begin{aligned}
&\nabla(\nabla h - G_R \nabla h G_A) + \nabla(G_R \nabla G_R)h + G_R \nabla G_R \nabla h \\
&\quad - h\nabla(G_A \nabla G_A) - \nabla h G_A \nabla G_A + i\epsilon([G_R, \tau_3]h - h[G_A, \tau_3]) \\
&\quad + 2[G, B]_K \Theta_S(x) = 0.
\end{aligned}
\tag{A3}
$$

Now, adding and subtracting $2([G,B]_R h - h[G,B]_A)\Theta_s(x)$ and rearranging the terms this can be written as

$$\nabla(\nabla h - G_R \nabla h G_A) + (\nabla(G_R \nabla G_R) + i\epsilon[G_R,\tau_3] + 2[G,B]_R \Theta_s(x))h$$
$$+ G_R \nabla G_R \nabla h - h(\nabla(G_A \nabla G_A) + i\epsilon[G_A,\tau_3] + 2[G,B]_A)$$
$$- \nabla h G_A \nabla G_A + 2([G,B]_K - [G,B]_R h + h[G,B]_A)\Theta_s(x) = 0.$$
(A4)

Now, using the retarded and advanced components two of these expressions can be seen to vanish, and the equation left is

$$0 = \nabla(\nabla h - G_R \nabla h G_A) + G_R \nabla G_R \nabla h - \nabla h G_A \nabla G_A$$
$$+ 2([G,B]_K - [G,B]_R h + h[G,B]_A)\Theta_s(x).$$
$$= \nabla(\nabla h - G_R \nabla h G_A) + G_R \nabla G_R \nabla h - \nabla h G_A \nabla G_A + S = 0,$$
$$S = 2([G,B]_K - [G,B]_R h + h[G,B]_A)\Theta_s(x).$$
(A5)

$$G_R \tau_3 G_R^\dagger \tau_3 = \begin{bmatrix} |\cosh\theta|^2 - |\sinh\theta|^2 e^{-2\mathrm{Im}\chi} & \cosh\theta\sinh\theta^* e^{i\chi^*} - \cosh\theta^* \sinh\theta e^{i\chi} \\ \cosh\theta\sinh\theta^* e^{-i\chi^*} - \cosh\theta^* \sinh\theta e^{-i\chi} & |\cosh\theta|^2 - |\sinh\theta|^2 e^{2\mathrm{Im}\chi} \end{bmatrix}$$
(A9)

Thus, define

$$D_L = \mathrm{Tr}(1 - G_R G_A) = 2 + 2|\cosh\theta|^2$$
$$- 2|\sinh\theta|^2 \cosh 2\mathrm{Im}\chi,$$
(A10)

$$G_R G_R^\dagger \tau_3 = \begin{bmatrix} \cosh\theta & \sinh\theta e^{i\chi} \\ -\sinh\theta e^{-i\chi} & -\cosh\theta \end{bmatrix} \begin{bmatrix} \cosh\theta^* & \sinh\theta^* e^{i\chi^*} \\ \sinh\theta^* e^{-i\chi^*} & \cosh\theta^* \end{bmatrix}$$
$$= \begin{bmatrix} |\cosh\theta|^2 + |\sinh\theta|^2 e^{-2\mathrm{Im}\chi} & \cosh\theta\sinh\theta^* e^{i\chi^*} + \cosh\theta^* \sinh\theta e^{i\chi} \\ -\cosh\theta\sinh\theta^* e^{-i\chi^*} - \cosh\theta^* \sinh\theta e^{-i\chi} & -|\cosh\theta|^2 - |\sinh\theta|^2 e^{2\mathrm{Im}\chi} \end{bmatrix}.$$
(A12)

Thus, define

$$C_L = \mathrm{Tr}(\tau_3 - G_R \tau_3 G_A) = -2|\sinh\theta|^2 \sinh 2\mathrm{Im}\chi = -C_T,$$
(A13)

and

$$D_T = \mathrm{Tr}(1 - \tau_3 G_R \tau_3 G_A)$$
$$= 2 + 2|\cosh\theta|^2 + 2|\sinh\theta|^2 \cosh 2\mathrm{Im}\chi.$$
(A14)

Now writing $h = f_L \tau_0 + f_T \tau_3$ this becomes

$$\nabla((1 - G_R G_A)\nabla f_L) + \nabla((\tau_3 - G_R \tau_3 G_A)\nabla f_T)$$
$$+ \nabla f_L(G_R \nabla G_R - G_A \nabla G_A) + \nabla f_T(G_R \nabla G_R \tau_3 - \tau_3 G_A \nabla G_A)$$
$$+ S = 0.$$
(A6)

Now, the terms in equation (A6) need to be calculated.

A.1. Calculation of terms

The first term in equation (A6) is $1 - G_R G_A = 1 + G_R \tau_3 G_R^\dagger \tau_3$. Using that

$$G_R = \begin{bmatrix} \cosh\theta & \sinh\theta e^{i\chi} \\ -\sinh\theta e^{-i\chi} & -\cosh\theta \end{bmatrix},$$
(A7)

it follows that

$$\tau_3 G_R^\dagger \tau_3 = \begin{bmatrix} \cosh\theta^* & \sinh\theta^* e^{i\chi^*} \\ -\sinh\theta^* e^{-i\chi^*} & -\cosh\theta^* \end{bmatrix},$$
(A8)

and therefore that

and

$$C_T = \mathrm{Tr}(\tau_3 - \tau_3 G_R G_A) = 2|\sinh\theta|^2 \sinh 2\mathrm{Im}\chi.$$
(A11)

For the second term note that $-G_R \tau_3 G_A = G_R G_R^\dagger \tau_3$. This can be calculated and yields

The third term reads $G_R \nabla G_R \tau_3 - \tau_3 G_A \nabla G_A$. Now,

$$G_R \nabla G_R = \begin{bmatrix} 0 & e^{i\chi} \\ e^{-i\chi} & 0 \end{bmatrix} \frac{\partial\theta}{\partial x}$$
$$+ \begin{bmatrix} i\sinh^2\theta & i\cosh\theta\sinh\theta e^{i\chi} \\ -i\cosh\theta\sinh\theta e^{-i\chi} & -i\sinh^2\theta \end{bmatrix} \frac{\partial\chi}{\partial x}.$$

From this it can be calculated that

$$\mathrm{Tr}(G_R \nabla G_R) = 0,$$

$$\mathrm{Tr}(\tau_3 G_R \nabla G_R) = 2i \sinh^2 \theta \frac{\partial \chi}{\partial x}. \qquad (A15)$$

Similarly, for $G_A \nabla G_A$

$$G_A \nabla G_A = \begin{bmatrix} 0 & e^{i\chi^*} \\ e^{-i\chi^*} & 0 \end{bmatrix} \frac{\partial \theta^*}{\partial x}$$

$$+ \begin{bmatrix} i \sinh^2 \theta^* & i \cosh \theta^* \sinh \theta^* e^{i\chi^*} \\ -i \cosh \theta^* \sinh \theta^* e^{-i\chi^*} & -i \sinh^2 \theta^* \end{bmatrix} \frac{\partial \chi^*}{\partial x}.$$

From this it can be calculated that

$$\mathrm{Tr}(G_A \nabla G_A) = 0,$$

$$\mathrm{Tr}(\tau_3 G_A \nabla G_A) = 2i \sinh^2 \theta^* \frac{\partial \chi^*}{\partial x}. \qquad (A16)$$

From equations (A15) and (A16) it now follows that

$$\mathrm{Tr}(G_R \nabla G_R - G_A \nabla G_A) = 0.$$

$$\mathrm{Tr}(\tau_3 (G_R \nabla G_R - G_A \nabla G_A)) = 2i \sinh^2 \theta \frac{\partial \chi}{\partial x} - 2i \sinh \theta^* \frac{\partial \chi^*}{\partial x}$$

$$= -4 \mathrm{Im} \left(\sinh^2 \theta \frac{\partial \chi}{\partial x} \right).$$

This latter quantity is defined as *ImIs*.

A.2. Parametrised Keldysh equation

With the expressions from the previous section (A10), (A11), (A13) and (A14) the Keldysh differential equation (A6) can be put in parametrised form. Taking the trace of (A6) gives

$$\nabla(D_L \nabla f_L) + \nabla(C_L \nabla f_T) + ImIs \nabla f_T + \mathrm{Tr}(S) = 0. \qquad (A18)$$

The second equation is found by taking the trace of (A6) after multiplying by τ_3. This gives

$$\nabla(D_T \nabla f_T) + \nabla(C_T \nabla f_L) + ImIs \nabla f_L + \mathrm{Tr}(\tau_3 S) = 0. \qquad (A19)$$

Compared with expressions in literature [15, 20], there is one extra term in each equation, $\nabla(C_L \nabla f_T)$ and $\nabla(C_T \nabla f_L)$. Now, these terms are proportional to $\sinh 2 \mathrm{Im} \chi$, which means that they vanish if χ is real. Thus, in case χ is real the equations presented in [15, 20] are recovered.

Appendix B. Boundary condition

In this section the Tanaka Nazarov boundary conditions will be calculated for the VT junction. The derivation will start from equation (9) of [34]. The boundary condition can be expressed as

$$G \frac{\partial}{\partial y} G = \sum_n I_n, \qquad (B1)$$

where

$$I_n = 2[G, B_n]$$

$$B_n = \left(-T_{1n}[G_1, H_-^{-1}] + H_-^{-1} H_+ - T_{1n}^2 G_1 H_-^{-1} H_+ G_1 \right)^{-1}$$

$$\times \left(T_{1n}(1 - H_-^{-1}) + T_{1n} G_1 H_-^{-1} H_+ \right). \qquad (B2)$$

In this equation G_1 is the Green's function in the normal metal, $H_\pm = \frac{1}{2}(G_{2+} \pm G_{2-})$, where $G_{2\pm}$ are Green's functions in the superconductor with $+,-$ indicating direction of motion towards or away from the interface. A problem with the direct calculation of expression (B2) is that it contains H_-^{-1}. In conventional superconductors $H_- = 0$ and in superconductors it is possible $H_- \approx 0$ for several channels as well. For that reason, B_n is rewritten as

$$B_n = \left(-T_{1n}[G_1, H_-^{-1}] + H_-^{-1} H_+ - T_{1n}^2 G_1 H_-^{-1} H_+ G_1 \right)^{-1}$$

$$\times (H_+^{-1} H_-)^{-1} (H_+^{-1} H_-) \left(T_{1n}(1 - H_-^{-1}) + T_{1n} G_1 H_-^{-1} H_+ \right)$$

$$= \left(-T_{1n} H_+^{-1} H_- G_1 H_-^{-1} H_+ H_+^{-1} + T_{1n} H_+^{-1} G_1 \right.$$

$$\left. + 1 - T_{1n}^2 H_+^{-1} H_- G_1 H_-^{-1} H_+ G_1 \right)^{-1}$$

$$\times \left(T_{1n}(H_+^{-1} H_- - H_+^{-1}) + T_{1n} H_+^{-1} H_- G_1 H_-^{-1} H_+ \right). \qquad (B3)$$

In this last expression H_-^{-1} is still present, but only in the combination $H_+^{-1} H_- G_1 H_-^{-1} H_+ = H_+^{-1} H_- G_1 (H_+^{-1} H_-)^{-1}$. It is this latter expression that can be used for both the retarded and Keldysh component.

B.1. Retarded component

The following derivation holds in case the superconducting order parameter in the superconducting electrodes is $\Delta = \Delta_0$ or $\Delta = \Delta_0 \cos \phi - \alpha$, where ϕ is the angle made with the surface and α is the angular mismatch between electrodes and normal metal.

The retarded component of B_n is

$$B_R = \left(-T_{1n} R_p^{-1} R_m G_1 (R_p^{-1} R_m)^{-1} + T_{1n} R_p^{-1} G_1 \right.$$

$$\left. + 1 - T_{1n}^2 R_p^{-1} R_m G_1 (R_p^{-1} R_m)^{-1} G_1 \right)^{-1}$$

$$\times \left(T_{1n} R_p^{-1} R_m - T_{1n} R_p^{-1} + T_{1n}^2 R_p^{-1} R_m G_1 (R_p^{-1} R_m)^{-1} \right). \qquad (B4)$$

We can write

$$G_{2\pm} = \begin{bmatrix} g_\pm & f_\pm e^{i\psi} \\ -f_\pm e^{-i\psi} & -g_\pm \end{bmatrix}, \qquad (B5)$$

where ψ is the superconducting phase of the electrode. Therefore

$$R_p = \frac{1}{2} \begin{bmatrix} g_+ + g_- & (f_+ + f_-) e^{i\psi} \\ -(f_+ + f_-) e^{-i\psi} & -(g_+ + g_-) \end{bmatrix} \qquad (B6)$$

$$R_p^{-1} = \frac{1}{1 + g_+ g_- - f_+ f_-} \begin{bmatrix} g_+ + g_- & (f_+ + f_-)e^{i\psi} \\ -(f_+ + f_-)e^{-i\psi} & -(g_+ + g_-) \end{bmatrix},$$
(B7)

$$R_m = \frac{1}{2} \begin{bmatrix} g_+ - g_- & (f_+ - f_-)e^{i\psi} \\ -(f_+ - f_-)e^{-i\psi} & -(g_+ - g_-) \end{bmatrix}.$$
(B8)

With this, $R_p^{-1} R_m$ can be calculated. Using that $g_+^2 - f_+^2 = g_-^2 - f_-^2 = 1$ and $(g_+ + g_-)(f_+ - f_-) - (g_+ - g_-)(f_+ + f_-) = g_+ f_+ - g_+ f_- + g_- f_+ - g_- f_- - g_+ f_+ - g_+ f_- + g_- f_+ + g_- f_- = 2(g_- f_+ - g_+ f_-)$, it follows that

$$R_p^{-1} R_m = \frac{g_- f_+ - g_+ f_-}{1 + g_+ g_- - f_+ f_-} \begin{bmatrix} 0 & e^{i\psi} \\ e^{-i\psi} & 0 \end{bmatrix}$$

$$= A \begin{bmatrix} 0 & e^{i\psi} \\ e^{-i\psi} & 0 \end{bmatrix} = A\Psi,$$
(B9)

where $A = \frac{g_- f_+ - g_+ f_-}{1 + g_+ g_- - f_+ f_-}$ and $\Psi = \begin{bmatrix} 0 & e^{i\psi} \\ e^{-i\psi} & 0 \end{bmatrix}$. But then

$$R_p^{-1} R_m G_1 (R_p^{-1} R_m)^{-1} = A \begin{bmatrix} 0 & e^{i\psi} \\ e^{-i\psi} & 0 \end{bmatrix} G_1 \frac{1}{A} \begin{bmatrix} 0 & e^{i\psi} \\ e^{-i\psi} & 0 \end{bmatrix}$$

$$= \begin{bmatrix} 0 & e^{i\psi} \\ e^{-i\psi} & 0 \end{bmatrix} G_1 \begin{bmatrix} 0 & e^{i\psi} \\ e^{-i\psi} & 0 \end{bmatrix}$$

$$= \Psi G_1 \Psi.$$
(B10)

With this B_R can be expressed as

$$B_R = \left(-T_{1n}\Psi G_1 \Psi R_p^{-1} + T_{1n} R_p^{-1} G_1 + 1 - T_{1n}^2 \Psi G_1 \Psi G_1 \right)^{-1}$$
$$\times \left(T_{1n} R_p^{-1} R_m - T_{1n} R_p^{-1} + T_{1n} \Psi G_1 \Psi \right).$$
(B11)

This expression does not contain R_m^{-1} and can thus be computed using MATLAB.

A connection can be made to the expression found in [34]. Parametrising $G_1 = \begin{bmatrix} \cosh\theta & \sinh\theta e^{i\chi} \\ -\sinh\theta e^{-i\chi} & -\cosh\theta \end{bmatrix}$ as in [15], $\Psi G_1 \Psi$ can be calculated as follows:

$$\Psi G_1 \Psi = \begin{bmatrix} 0 & e^{i\psi} \\ e^{-i\psi} & 0 \end{bmatrix} \begin{bmatrix} \cosh\theta & \sinh\theta e^{i\chi} \\ -\sinh\theta e^{-i\chi} & -\cosh\theta \end{bmatrix} \begin{bmatrix} 0 & e^{i\psi} \\ e^{-i\psi} & 0 \end{bmatrix}$$

$$= \begin{bmatrix} 0 & e^{i\psi} \\ e^{-i\psi} & 0 \end{bmatrix} \begin{bmatrix} \sinh\theta e^{i(\chi-\psi)} & \cosh\theta e^{i\psi} \\ -\cosh\theta e^{-i\psi} & -\sinh\theta e^{-i(\chi-\psi)} \end{bmatrix}$$

$$= \begin{bmatrix} -\cosh\theta & -\sinh\theta e^{-i(\chi-2\psi)} \\ \sinh\theta e^{i(\chi-\psi)} & \cosh\theta \end{bmatrix}$$

$$= -G_1 + 2i\sinh\theta\sin\chi - \psi \begin{bmatrix} 0 & e^{i\psi} \\ e^{-i\psi} & 0 \end{bmatrix}.$$

If the superconducting phases in the electrodes and the normal metal are the same, this reduces to $\Psi G_1 \Psi = -G_1$, and in that case equation (B11) reduces to the expression found in [34].

B.2. Keldysh component

The Keldysh component of the boundary condition can be expressed as follows:

$$I_K = 2([G, B_n])_K = 2(G^R B_K + G^K B_A - B_R G^K - B_K G^A).$$
(B13)

Now, B_R has been calculated in section B.1, and B_A can be calculated from $B_A = -\tau_3 B_R^\dagger \tau_3$, where τ_3 is the third Pauli matrix. Thus, only B_K needs to be calculated. From equation (B3) it can be read that $B = D^{-1}N$, where

$$D = \left(-T_{1n} H_+^{-1} H_- G_1 H_-^{-1} H_+ H_+^{-1} + T_{1n} H_+^{-1} G_1 \right.$$
$$\left. + 1 - T_{1n}^2 H_+^{-1} H_- G_1 H_-^{-1} H_+ G_1 \right)^{-1}$$

$$N = \left(T_{1n}(H_+^{-1} H_- - H_+^{-1}) + T_{1n} H_+^{-1} H_- G_1 H_-^{-1} H_+ \right). \quad \text{(B14)}$$

With this expression B_K can be expressed as

$$B_K = D_R^{-1} N_K - (D^{-1})_K N_A = D_R^{-1} N_K - D_R^{-1} D_K D_A^{-1} N_A.$$
(B15)

Following [34] $D_A^{-1} N_A = B_A$, which leaves only N_K and D_K to be calculated. In order to find these expressions, the Keldysh component of each of the terms of N and D will be calculated. In order to this, the distribution functions in the normal metal are denoted by h as before, those in the superconducting electrode by h_s:

$$(1)_K = 0.$$
$$(H_+^{-1})_K = -R_p^{-1} K_p A_p^{-1} = R_p^{-1} h_s - h_s A_p^{-1}.$$
$$(H_+^{-1} G_1)_K = R_p^1 G^K + (H_+^{-1})_K G^A$$
$$= R_p^1(R_1 h - hA_1) + (R_p^{-1} h_s - h_s A_p^{-1})A_1.$$
$$(H_+^{-1} H_-)_K = R_p^{-1}(H_-)_K + (H_+^{-1})_K A_m$$
$$= R_p^{-1} R_m h_s - R_p^{-1} h_s A_m + R_p^{-1} h_s A_m$$
$$\quad - h_s A_p^{-1} A_m$$
$$= R_p^{-1} R_m h_s - h_s A_p^{-1} A_m.$$
$$(H_+^{-1} H_- G_1 H_-^{-1} H_+ H_+^{-1})_K = (H_+^{-1} H_- G_1 H_-^{-1} H_+)_R (H_+^{-1})_K$$
$$\quad + (H_+^{-1} H_- G_1 H_-^{-1} H_+)_K A_p^{-1}$$
$$= \Psi R_1 \Psi (R_p^{-1} h_s - h_s A_p^{-1})$$
$$\quad + (H_+^{-1} H_- G_1 H_-^{-1} H_+)_K A_p^{-1}.$$
$$(H_+^{-1} H_- G_1 H_-^{-1} H_+ G_1)_K = (H_+^{-1} H_- G_1 H_-^{-1} H_+)_R G^K$$
$$\quad + (H_+^{-1} H_- G_1 H_-^{-1} H_+)_K A_1$$
$$= \Psi R_1 \Psi (R_1 h_s - h_s A_1)$$
$$\quad + (H_+^{-1} H_- G_1 H_-^{-1} H_+)_K A_1.$$

Substituting these expressions

$$D_K = -T_{1n}\Psi R_1 \Psi(R_p^{-1} h_s - h_s A_p^{-1}) + T_{1n} R_p^{-1}(R_1 h - hA_1)$$
$$\quad - T_{1n}(H_+^{-1} H_- G_1 H_-^{-1} H_+)_K A_p^{-1} + T_{1n}(R_p^{-1} h - hA_p^{-1})A_1$$
$$\quad - T_{1n}^2 \Psi R_1 \Psi(R_1 h - hA_1) - T_{1n}^2 (H_+^{-1} H_- G_1 H_-^{-1} H_+)_K A_1.$$
(B16)

and

$$N_K = T_{1n}R_p^{-1}R_m h_s - T_{1n}h_s A_p^{-1}A_m - T_{1n}R_p^{-1}h_s + T_{1n}h_s A_p^{-1}$$
$$+ T_{1n}^2(H_+H_-G_1H_-^{-1}H_+)_K. \tag{B17}$$

This leaves only $(H_+H_-G_1H_-^{-1}H_+)_K$ to calculate. To this end, first observe that

$$A_m^{-1}A_p = (-\tau_3(R_m^{-1})^\dagger\tau_3)(-\tau_3 R_p\tau_3) = \tau_3(R_m^{-1})^\dagger R_p^\dagger\tau_3$$
$$= \tau_3(R_p R_m^{-1})^\dagger\tau_3. \tag{B18}$$

Using that H_+ and H_-^{-1} anticommute it follows that

$$A_m^{-1}A_p = -\tau_3(R_m^{-1}R_p)^\dagger\tau_3 = -\frac{1}{A}\tau_3\Psi\tau_3 = \frac{1}{A}\Psi, \tag{B19}$$

where it was used that Ψ is a Hermitian matrix and that its diagonal elements vanish.

Thus,

$$R_p^{-1}R_m G_1 A_m^{-1}A_p = \frac{A}{A^*}\Psi G_1\Psi. \tag{B20}$$

Now the remaining term can be calculated:

$$(H_+H_-G_1H_-^{-1}H_+)_K = (H_+H_-)_K A_1(H_-^{-1}H_+)_A$$
$$+ (H_+H_-)_R(R_1 h - hA_1)(H_-^{-1}H_+)_A$$
$$+ (H_+H_-)_R R_1(H_-^{-1}H_+)_K.$$

As calculated before, $(H_+^{-1}H_-)_K = R_p^{-1}R_m h_s - h_s A_p^{-1}A_m$. Thus,

$$(H_+H_-)_K A_1(H_-^{-1}H_+)_A = R_p^{-1}R_m h_s A_1 A_m^{-1}A_p - h_s A_p^{-1}A_m A_1 A_m^{-1}A_p$$
$$= \frac{A}{A^*}\Psi h_s A_1\Psi - h_s\Psi A_1\Psi.$$
$$(H_+H_-)_R K_1(H_-^{-1}H_+)_A = R_p^{-1}R_m(R_1 h - hA_1)A_m^{-1}A_p$$
$$= \frac{A}{A^*}\Psi(R_1 h - hA_1)\Psi$$
$$(H_+H_-)_R R_1(H_-^{-1}H_+)_K = R_p^{-1}R_m R_1(R_m^{-1}R_p h_s - h_s A_m^{-1}A_p)$$
$$= \Psi R_1\Psi h_s - \frac{A}{A^*}\Psi R_1 h_s\Psi. \tag{B21}$$

With this the expression for $(H_+H_-G_1H_-^{-1}H_+)_K$ finally becomes

$$(H_+H_-G_1H_-^{-1}H_+)_K = \Psi R_1\Psi h_s - h_s\Psi A_1\Psi$$
$$+ \frac{A}{A^*}(\Psi R_1(h - h_s)\Psi - \Psi(h - h_s)A_1\Psi). \tag{B22}$$

With this an expression for all terms of B_K has been found and I_K can be calculated.

Appendix C. Analytical considerations

In this section a linearisation of the Usadel, valid under the assumption of a small proximity effect and a small phase difference, is studied to improve understanding of the behaviour of the spectral supercurrent.

The Usadel equation in the region in between the electrodes reads in absence of a phase difference

$$\frac{\partial^2\theta}{\partial x^2} + 2i\alpha\epsilon\sinh\theta = 0. \tag{C1}$$

Now, in case the proximity effect is small, that is, $|\theta| \ll 1$, this can be approximated by

$$\frac{\partial^2\theta}{\partial x^2} + 2i\alpha\epsilon\theta = 0. \tag{C2}$$

The symmetric solution to this equation reads

$$\theta(x,\epsilon) = \theta_0(\epsilon)\frac{\cosh\sqrt{-2i\alpha\epsilon}x}{\cosh\sqrt{-2i\alpha\epsilon}\frac{L}{2}}, \tag{C3}$$

where $\theta_0(\epsilon)$ is the value at the left and right endpoints of the interval under consideration, mainly determined by the superconducting electrodes. The value of θ_0 is thus not expected to have a strong length dependence.

From this it can be deduced that

$$\theta(0,\epsilon) = \theta_0\frac{1}{\cosh\sqrt{-2i\alpha\epsilon}\frac{L}{2}}, \tag{C4}$$

which shows that in case $\sqrt{\epsilon}L \gg 1$ the value of θ in the centre of the junction is suppressed by a complex exponential with $\sqrt{\epsilon}L$. In case of a nonzero phase difference the coupled equations should be considered. Again using the approximation $\sinh x \approx x$, the equations read

$$\frac{\partial^2\theta}{\partial x^2} + 2i\alpha\epsilon\theta - \left(\frac{\partial\chi}{\partial x}\right)^2\theta = 0. \tag{C5}$$

$$\frac{\partial}{\partial x}\left(\theta^2\frac{\partial\chi}{\partial x}\right) = 0. \tag{C6}$$

The second of these equations can be written as

$$\theta^2\frac{\partial\chi}{\partial x} = \frac{j_\epsilon}{2}, \tag{C7}$$

where j_ε is the position independent spectral supercurrent. Substituting this in the first equation one obtains

$$\frac{\partial^2\theta}{\partial x^2} + 2i\alpha\epsilon\theta - \frac{j_\epsilon^2}{4\theta^4}\theta = 0. \tag{C8}$$

Now suppose that the second term completely dominates the third over the entire interval. This is the case if the current through the junction is small enough, that is, if the phase difference between the electrodes is small enough. In this approximation, the solution to the θ-equation is expression (C3). Substituting this in the second equation, and considering that the

phase difference between the ends of the intervals is $\Delta\psi$, one finds

$$\Delta\psi = \int_{-\frac{L}{2}}^{\frac{L}{2}} \frac{\partial\chi}{\partial x} dx \tag{C9}$$

$$= \int_{-\frac{L}{2}}^{\frac{L}{2}} \frac{j_\epsilon}{2\theta^2} dx \tag{C10}$$

$$= \frac{j_\epsilon \cosh^2 \sqrt{2i\alpha\epsilon} \frac{L}{2}}{2\theta_0^2} \int_{-\frac{L}{2}}^{\frac{L}{2}} \frac{1}{\cosh^2 \sqrt{2i\alpha\epsilon} x} dx. \tag{C11}$$

As indicated, this is in the regime $\sqrt{\epsilon}L \gg 1$, so the integration limits can be replaced by $\pm\infty$ and the integral yields a factor $2\sqrt{2i\epsilon}$. Thus, the phase difference and the spectral supercurrent are related by

$$j_\epsilon \approx \frac{\Delta\psi\theta_0^2 \sqrt{-2i\alpha\epsilon}}{\cosh^2 \sqrt{2i\alpha\epsilon} \frac{L}{2}}.$$

ORCID iD

T H Kokkeler https://orcid.org/0000-0001-8681-3376

References

[1] Onnes H K 1911 Further experiments with liquid helium *Proc. KNAW* vol 13 pp 1910–1

[2] London F and London H 1935 The electromagnetic equations of the supraconductor *Proc. R. Soc.* A **149** 71

[3] Ginzburg V L 2004 On superconductivity and superfluidity (what I have and have not managed to do), as well as on the 'physical minimum' at the beginning of the XXI century (December 8, 2003) *Phys.-Usp.* **47** 1155

[4] Bardeen J, Cooper L N and Schrieffer J R 1957 Microscopic theory of superconductivity *Phys. Rev.* **106** 162

[5] Josephson B 1962 Possible new effects in superconductive tunnelling *Phys. Lett.* **1** 251

[6] Yanson I, Svistunov V and Dmitrenko I 1965 Experimental observation of the tunnel effect for cooper pairs with the emission of photons *Sov. Phys - JETP* **21** 650

[7] Schmidt V 1997 *The Physics of Superconductors* ed P Müller and A V Ustinov (Berlin: Springer) (https://doi.org/10.1007/978-3-662-03501-6_7)

[8] Steglich F, Aarts J, Bredl C, Lieke W, Meschede D, Franz W and Schäfer H 1979 Superconductivity in the presence of strong pauli paramagnetism: CeCu$_2$Si$_2$ *Phys. Rev. Lett.* **43** 1892

[9] Bednorz J G and Müller K A 1986 Possible high T$_c$ superconductivity in the Ba–La–Cu–O system *Z. Phys.* B **64** 189

[10] Sigrist M 2005 Review on the chiral p-wave phase of Sr$_2$RuO$_4$ *Prog. Theor. Phys. Suppl.* **160** 1

[11] Maeno Y, Kittaka S, Nomura T, Yonezawa S and Ishida K 2012 Evaluation of spin-triplet superconductivity in Sr$_2$RuO$_4$ *J. Phys. Soc. Japan* **81** 011009

[12] Hilgenkamp H, Smilde A, Smilde H-J H, Blank D H A, Rijnders G, Rogalla H, Kirtley J R and Tsuei C C 2003 Ordering and manipulation of the magnetic moments in large-scale superconducting π-loop arrays *Nature* **422** 50

[13] Kitaev A 2001 Unpaired Majorana fermions in quantum wires *Phys.-Usp.* **44** 131

[14] Gorkov L 1958 On the energy spectrum of superconductors *Sov. Phys.—JETP* **7** 158

[15] Belzig W, Wilhelm F K, Bruder C, Schön G and Zaikin A 1999 Quasiclassical Green's function approach to mesoscopic superconductivity *Superlattices Microstruct.* **25** 1251

[16] Chandrasekhar V 2004 An introduction to the quasiclassical theory of superconductivity for diffusive proximity-coupled systems *The Physics of Superconductors* ed K-H Bennemann and J Ketterson (Berlin: Springer) pp 55–110

[17] Likharev K 1979 Superconducting weak links *Rev. Mod. Phys.* **51** 101

[18] Golubov A A, Kupriyanov M Y and Il'ichev E 2004 The current-phase relation in Josephson junctions *Rev. Mod. Phys.* **76** 411

[19] Ishii C 1972 Thermodynamical properties of Josephson junction with a normal metal barrier *Prog. Theor. Phys.* **47** 1464

[20] Brinkman A, Golubov A, Rogalla H, Wilhelm F and Kupriyanov Y 2003 Microscopic nonequilibrium theory of double-barrier Josephson junctions *Phys. Rev.* B **68** 224513

[21] Zhou F, Charlat P, Spivak B and Pannetier B 1998 Density of states in superconductor–normal metal–superconductor junctions *J. Low Temp. Phys.* **110** 841

[22] Ivanov D A, von Roten R and Blatter G 2002 Minigap in a long disordered SNS junction: analytical results *Phys. Rev.* B **66** 052507

[23] Volkov A F and Eremin I M 2021 Proximity induced spontaneous currents and phase transition in superconductor/normal metal heterostructures (arXiv:2102.04870)

[24] Fominov Y V and Feigel'man M 2001 Superconductive properties of thin dirty superconductor-normal-metal bilayers *Phys. Rev.* B **63** 094518

[25] Volkov A and Takayanagi H 1996 Effect of gate voltage on critical current in controllable superconductor-normal-metal-superconductor Josephson junctions *Phys. Rev.* B **53** 15162

[26] Volkov A and Takayanagi H 1997 Long-range phase-coherent effects in the transport properties of mesoscopic superconductor-normal-metal structures *Phys. Rev.* B **56** 11184

[27] Toyoda E, Takayanagi H and Nakano H 1999 Systematic gate-controlled reentrant conductance of a superconductor-semiconductor two-dimensional electron gas junction *Phys. Rev.* B **59** R11653

[28] Shaikhaidarov R, Volkov A, Takayanagi H, Petrashov V and Delsing P 2000 Josephson effects in a superconductor-normal-metal mesoscopic structure with a dangling superconducting arm *Phys. Rev.* B **62** R14649

[29] Suzuki S-I, Golubov A, Asano Y and Tanaka Y 2019 Effects of phase coherence on local density of states in superconducting proximity structures *Phys. Rev.* B **100** 024511

[30] Tanaka Y, Kashiwaya S and Yokoyama T 2005 Theory of enhanced proximity effect by midgap Andreev resonant state in diffusive normal-metal/triplet superconductor junctions *Phys. Rev.* B **71**

[31] Tanaka Y and Kashiwaya S 2004 Anomalous charge transport in triplet superconductor junctions *Phys. Rev.* B **70**

[32] Nazarov Y V 1999 Novel circuit theory of Andreev reflection *Superlattices Microstruct.* **25** 1221

[33] Tanaka Y, Nazarov Y and Kashiwaya S 2003 Circuit theory of unconventional superconductor junctions *Phys. Rev. Lett.* **90** 167003

[34] Tanaka Y, Nazarov Y V, Golubov A and Kashiwaya S 2004 Theory of charge transport in diffusive normal metal/unconventional singlet superconductor contacts *Phys. Rev.* B **69** 144519

[35] Suzuki S-I, Golubov A, Asano Y and Tanaka Y 2020 Quasiparticle spectrum in mesoscopic superconducting junctions with weak magnetization *Proc. Int. Conf. on Strongly Correlated Electron Systems (SCES2019)* p 011045

[36] Asano Y, Tanaka Y, Golubov A A and Kashiwaya S 2007 Conductance spectroscopy of spin-triplet superconductors *Phys. Rev. Lett.* **99** 067005

[37] Wilhelm F K, Schön G and Zaikin A D 1998 Mesoscopic superconducting-normal metal-superconducting transistor *Phys. Rev. Lett.* **81** 1682

[38] Eilenberger G 1968 Transformation of Gorkov's equation for type II superconductors into transport-like equations *Z. Phys.* A **214** 195

[39] Larkin A and Ovchinnikov Y 1975 Nonlinear conductivity of superconductors in the mixed state *Sov. Phys.—JETP* **41** 960

[40] Usadel K D 1970 Generalized diffusion equation for superconducting alloys *Phys. Rev. Lett.* **25** 507

[41] Schmid A and Schön G 1975 Linearized kinetic equations and relaxation processes of a superconductor near T_c *J. Low Temp. Phys.* **20** 207

[42] Fermi E I 1926 On the quantisation of the monatomic ideal gas *Rend. Lincei* (Translated to English by Zannoni A) **3** 9

[43] Dirac P A M 1926 On the theory of quantum mechanics *Proc. R. Soc.* A **112** 661

[44] Heikkilä T T, Vänskä T and Wilhelm F K 2003 Supercurrent-induced Peltier-like effect in superconductor/normal-metal weak links *Phys. Rev.* B **67** 100502

[45] Bardeen J, Cooper L N and Schrieffer J R 1957 Theory of superconductivity *Phys. Rev.* **108** 1175

[46] Golubov A A, Wilhelm F and Zaikin A 1997 Coherent charge transport in metallic proximity structures *Phys. Rev.* B **55** 1123

[47] Shumeiko V, Bratus E and Wendin G 1997 Scattering theory of superconductive tunneling in quantum junctions *Low Temp. Phys.* **23** 181

[48] Argaman N 1999 Nonequilibrium Josephson-like effects in wide mesoscopic SNS junctions *Superlattices Microstruct.* **25** 861